High rate concentration measurement of molecular gas mixtures using a spatial detection technique

Vincent Loriot, Edouard Hertz, Bruno Lavorel, Olivier Faucher

High rate concentration measurement of molecular gas mixtures using a spatial detection technique

V. Loriot, E. Hertz, B. Lavorel, and O. Faucher

Laboratoire Interdisciplinaire Carnot de Bourgogne (ICB),
UMR 5209 CNRS-Université de Bourgogne, 9 Av. A. Savary, BP 47 870,
F-21078 Dijon Cedex, France[a)]

Concentration measurement in molecular gas mixtures using a snapshot spatial imaging technique is reported. The approach consists of measuring the birefringence of the molecular sample when field-free alignment takes place, each molecular component producing a signal with an amplitude depending on the molecular density. The concentration measurement is obtained on a single-shot basis by probing the time-varying birefringence through femtosecond time-resolved optical polarigraphy (FTOP). The relevance of the method is assessed in air.

PACS numbers: 37.10 Vz, 42.50 Hz, 42.50 Md

[a)]Electronic mail: edouard.hertz@u-bourgogne.fr

I. INTRODUCTION

Field-free molecular alignment by short laser pulses is a research field of great interest with a broad range of promising applications.[1] Quantum mechanically, the underlying mechanism behind this specific regime of alignment is well understood. A short (non-resonant) laser pulse excites a rotational wavepacket by driving a series of impulsive stimulated Raman transitions within the ground state of the molecule. The rotational wavepacket thus produced revives periodically in time with subsequent dephasing and rephasing giving rise to transient molecular alignment after the pulse turnoff.[2–4] Such manipulation of external degrees of freedom constitutes a promising application of quantum control by laser fields. Several works have investigated the use of control techniques as a spectroscopic tool to extract structural information regarding the molecule. Molecular phase[5] or potential energy curves[6] have been thus evaluated by analyzing the outcome of control experiment. In this regard, the field-free molecular alignment is particularly valuable. It has been applied for instance to provide tomographic imaging of molecular orbitals,[7] to extract the phase of high harmonic generation,[8] to analyze the angular dependence of strong field molecular ionization,[9–11] or to determine ionization probabilities.[12,13] A theoretical report has also proposed to exploit field-free molecular alignment in order to probe the collisions in dissipative media and determine the rate characterizing the elastic collisions.[14] In the present work, we explore the use of post-pulse molecular alignment as a diagnosis tool to measure, with a single-shot ability, the concentration of a molecular gas mixture. The relevance of the experimental scheme is assessed in atmospheric air with the measurement of O_2 and N_2 concentrations. While the method is based on probing the time-dependent birefringence as in previous reports,[15,16] the present work is conducted in a non perturbative regime where significant molecular alignment occurs. It aims at demonstrating that reliable diagnosis can be achieved under strong field regime and on a single-shot basis. To address the last issue, we emphasize that the large amplitude of signals associated to the present strong field spectroscopy is of crucial benefit allowing the implementation of a snapshot spatial imaging technique.[17,18]

II. PRINCIPLE AND EXPERIMENTAL SET-UP

The measurement that takes advantage of field-free molecular alignment can be described as follows. An ultrashort pump pulse, linearly polarized, interacts with a molecular gas sample. Post-pulse molecular alignment takes place and gives rise to a time-varying anisotropy of the sample measured with a delayed probe pulse. The amplitude of the birefringence signal depends on the molecular density. When considering a molecular gas mixture, the relative amplitude of signal associated to each molecular specie allows an evaluation of the concentration. The experimental scheme for a single-shot measurement of the time-varying birefringence is depicted in Fig. 1. The laser is a Ti:sapphire oscillator followed by a chirped pulse amplification stage providing 100 fs pulse duration with a maximum energy of 1 mJ at a 1 kHz repetition rate. A weak "probe" beam is produced using a reflection on a glass plate (GP). The transmitted beam, i.e. the "pump" beam, is polarized along the z axis with a polarizer (P_1), and a half-wave plate ($\lambda/2$) is used to adjust its energy. Typical energy for pump and probe beams are respectively 200-250 μJ and 20-25 μJ. The pump is focused in atmospheric air along the y axis with a lens (L_P) of 50 cm focal length. The probe pulse can be time-delayed with respect to the pump by a delay line (DL). After passing through a polarizer (P_2) that sets its field vector at 45° with respect to the z axis, the collimated probe beam intersects at a right angle the focused pump beam. When molecular alignment induced by the pump pulse occurs, the refractive index along the y and z directions becomes different. The birefringence of the medium modifies the probe polarization which is analyzed by the analyzer (A) crossed with respect to (P_2). The birefringence signal passing through the analyzer is collected with a system made of two lenses (L_1 and L_2) of 20 cm focal length that images the overlapping region of the two beams onto a charge-coupled device (CCD) of chip size 13.7 mm × 10.4 mm and pixel size 6.7 μm × 6.7 μm. The magnification factor of the imager is M=-1.02 and the depth of field $d_f \approx 500$ μm is much larger than the pump beam waist. The present arrangment allows a single-shot measurement of the birefringence induced by molecular alignment.[17] In fact, the cross beam geometry converts the time information into a spatial coordinate of the image. During its propagation, the pump pulse interacts with the molecules at different times with respect to their y-positions. The temporal response of the molecules excited by the pump is thus parameterized by the probe pulse along the spatial y coordinate of the image. For a suitable detection window,

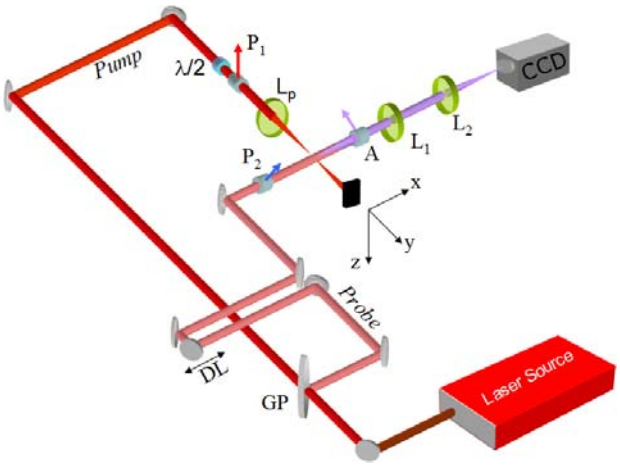

FIG. 1. (Color online) Experimental setup. (see text)

the confocal parameter b of the pump beam must be large enough to keep the axial intensity of the pump almost constant over the measurement region (here about 5 mm compared to $b \approx 10$ mm). While the principle of the measurement can be explained in this simple way, a more complete description including the spatial distribution of the two beams as well as the propagation of the probe over the transverse profile of the pump beam is required to suitably compute the signal captured by the CCD camera. Such analysis is detailed in the next section.

III. THEORY

In the following, our discussion will be limited to the case of linear molecules (only considered in the present work). For sake of clarity, we will focus first the discussion on the pure molecular sample whereas the case of gas mixtures will be examined at the end of the section. We use the expectation value $\langle \cos^2\theta \rangle(t)$, with θ the angle between the polarization axis and the internuclear axis, to characterize the degree of molecular alignment. When $\langle \cos^2\theta \rangle(t) > 1/3$, the molecular axis is preferentially aligned along the pump polarization axis. $\langle \cos^2\theta \rangle(t) < 1/3$ corresponds to a planar delocalization with the molecular axis preferentially distributed into the plane perpendicular to the polarization axis. An isotropic angular distribution of the molecules gives $\langle \cos^2\theta \rangle(t) = 1/3$. We point out that the amplitude but also the temporal shape of $\langle \cos^2\theta \rangle(t)$ depends on the field parameters (intensity, pulse shape, and polarization).[3,19,20] The pump and probe electric fields are considered to

have temporal Gaussian shapes with a pulse duration τ_{p}=100 fs. The probe beam profile is measured experimentally as explained below. When focusing our pump beam, we have noticed a small difference of beam radius along the x and z directions at the focus (coming from a slight astigmatism). In order to take into account this effect, the intensity of the pump beam propagating along y is described by the following expression

$$I_{\mathrm{p}}(x,y,z,t) = I_{0\mathrm{p}} \exp\left(-2(\tfrac{x^2}{w_{0x}^2} + \tfrac{z^2}{w_{0z}^2})\right) \times \exp\left(-4\ln 2\left(\tfrac{t-y/c}{\tau_{\mathrm{p}}}\right)^2\right), \quad (1)$$

with $I_{0\mathrm{p}}$ the peak intensity, w_{0x} and w_{0z} the beam waist along x and z, respectively. We have neglected in the above expression the variation of the intensity along y (i.e. we have fixed $w_x(y)$=w_{0x} and $w_z(y)$=w_{0z}). This approximation, which limits the computation time, is valid considering the large confocal parameters of the pump beam. The origin of time t is chosen to center the pulse at y=0. The interaction of molecules with this pulse leads to a space- and time-dependent alignment $\langle\cos^2\theta\rangle(x,y,z,t)$. The dependency of $\langle\cos^2\theta\rangle$ upon x, y, z accounts for the spatial intensity distribution of the pump as well as for its propagation through the term $t-y/c$ in Eq. 1. The molecular alignment leads to a transient birefringence $\Delta n = n_z - n_y$:

$$\Delta n(x,y,z,t) = \frac{3N}{4n\epsilon_0}\Delta\alpha\left(\left\langle\cos^2\theta\right\rangle(x,y,z,t) - \frac{1}{3}\right), \quad (2)$$

with n_z and n_y the refractive index respectively parallel and perpendicular to the pump polarization direction. n is the average value of the refractive index at the probe frequency, $\Delta\alpha$ the polarizability anisotropy,[21] N the number density, and ϵ_0 the dielectric constant of vacuum. The quantity $\langle\cos^2\theta\rangle$ is calculated from the numerical simulation of the time-dependent Schrödinger equation.[3] The image given by the CCD camera is related to the birefringence Δn detected by the time-delayed probe field E_{pr} propagating along x and can be written as

$$\mathcal{S}(y_c,z_c,\tau_0) \propto \int_{-\infty}^{\infty} dt \left\{\int_{-\infty}^{\infty} dx\ E_{\mathrm{pr}}(x,y,z,t-\tau_0-x/c) \times \Delta n\,(x,y,z,t)\right\}^2, \quad (3)$$

where y_c and z_c stand for the coordinates on the CCD camera related to the y and z coordinates by the relation y_c=$M\times y$ and z_c=$M\times z$. It should be noted that the negative

value of the magnification factor M leads to an inversion of the image. τ_0 denotes the pump-probe delay adjusted with the delay line. For sake of clarity, we analyze first the signal for the particular horizontal cut z=0 of the image considering the molecular sample as infinitely thin and located at x=0, i.e. x=z=0 in Eqs.1-3. We assume furthermore a spatially uniform probe beam. The signal is given in this case by the simplified expression

$$\mathcal{S}(y_c, \tau_0) \propto \int_{-\infty}^{\infty} I_{\rm pr}(t-\tau_0) \times \Delta n^2(y,t) dt, \tag{4}$$

with $I_{\rm pr}$ the probe intensity. If the confocal parameter b of the pump beam is large enough, the axial intensity of the pump is almost constant in the region of measurement. As a result, the dependency upon y of Δn relies only on the term $t - y/c$ of Eq. 1. In other words, the molecular alignment, and thus the birefringence, is of same amplitude in all points but time-delayed because "initiated" at a time rising like y. This birefringence being interrogated by the probe simultaneously for all y, the snapshot of the image vs y is equivalent to the signal obtained by tuning the delay τ with a conventional pump-probe method[3]

$$\mathcal{S}(\tau) \propto \int_{-\infty}^{\infty} I_{\rm pr}(t-\tau) \times \Delta n^2(t) dt, \tag{5}$$

with τ=τ_0-y/c. The method converts thus the time delay into the y coordinate. From this ideal one dimensional description, some insight can be gained into the influence of the other (x and z) dimensions. The z axis is along the transverse radius of the pump beam (see Fig. 1). The signal $\mathcal{S}(y_c)$ obtained from different horizontal cuts z_c reflects therefore the intensity distribution of the pump beam along z.[17] This properties can therefore provide access to the transverse profile of the pump beam and to possible spatial distortions arising from nonlinear effects. The role played by the last x coordinate is twofold. First, the probe beam propagates over the transverse profile of the pump. Since the depth of field d_f of the imaging system is much larger than the pump beam waist, the signal arises from the integration of the birefringence along x with molecules exposed to different intensities of the pump (see Eq. 3). This spatial effect could be limited by using a microscopic objective for reducing d_f. Second, the propagation of the probe pulse implies an additional temporal delay x/c in Eq. 3 confering to the relation τ=τ_0-y/c an "effective" character.

When a molecular mixture with K molecular species is investigated the signal of Eq.3

writes as:

$$\mathcal{S}(y_c, z_c, \tau_0) \propto \int_{-\infty}^{\infty} dt \left\{ \int_{-\infty}^{\infty} dx \; E_{\mathrm{pr}}(x, y, z, t - \tau_0 - x/c) \right. \\ \left. \times \sum_{i=1}^{K} N_i \Delta\alpha_i \Big(\left\langle \cos^2\theta \right\rangle_i (x, y, z, t) - \frac{1}{3} \Big) \right\}^2 . \quad (6)$$

Analysis of Eq. 6 indicates that each molecular component of the mixture produces its own temporal signal whose amplitude depends on the degree of alignment, the polarizability anisotropy, and the partial density. Knowing the polarizability anisotropy, the degree of alignment can be calculated and the overall signal fitted to extract the partial density of molecular components. The polarizability anisotropy can be determined if needed by means of a reference mixture of known concentration.[15] We point out that signal of Eq. 6 is proportional to the square of the total birefringence. When alignment revivals of different molecular species overlap in time, macroscopic interferences (corresponding to the cross terms) take place. These interferences lead to an enhanced sensitivity of the resulting transient shape with respect to the concentration.[15,16]

IV. RESULTS AND DISCUSSION

The relevance of the method is demonstrated by determining the concentration of N_2 and O_2 in atmospheric air. It is noticed that atoms are not detected by the present technique. Furthermore, the present technique is not suited for detecting molecular traces like CO_2 or H_2O. The N_2 and O_2 relative concentrations are thus C(N_2)=0.7884 and C(O_2)=0.2116 respectively. A typical image averaged over 90 laser shots (i.e. 90 ms considering the repetition rate of our laser system) is displayed in Fig. 2(a). The pump-probe delay was set around τ_0=10 ps. One of the advantage featured by the FTOP technique relies on the large temporal window covered by a single snapshot.[17] The temporal window in the present image is about 18 ps (see Fig. 2(b)).

In order to obtain the concentration, the signal from z_c-line=-6 to +6 of a given image is fitted with Eq. 6. As an illustration, the signal for the horizontal central cut (z_c-line=0) is depicted in Fig. 2(b) (full line) with the fit shown as mirror. For each line, apart from the relative N_2 concentration, the fitted parameters are a scaling factor, the pump-probe delay τ_0, the beam waist w_{0x}, and the peak intensity $I_{0\mathrm{p}}$ (see Eq. 1). The beam waist w_{0z}=39 μm

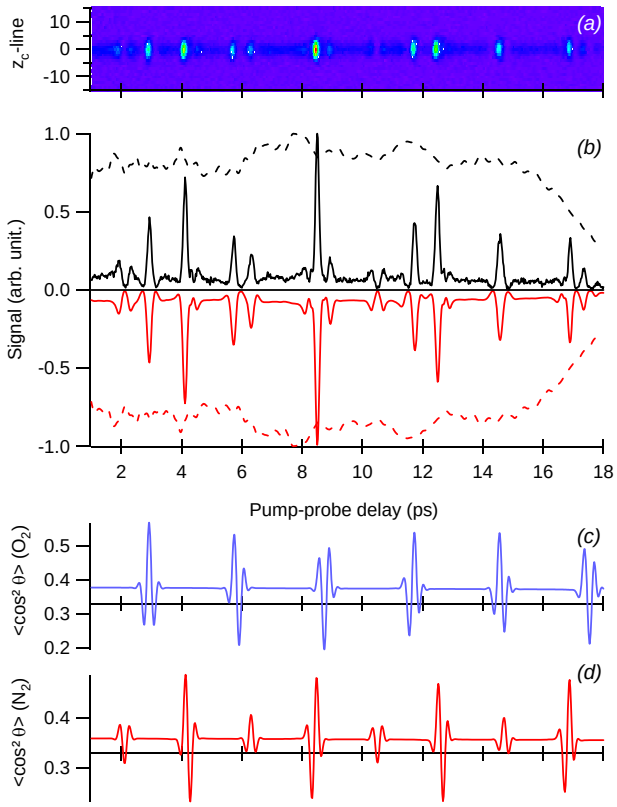

FIG. 2. (Color online) (a) FTOP image recorded in atmospheric air. (b) Signal (full line) from the horizontal central line (z_c=0) of the image. Fitted signal is shown reversed and the measured probe beam profile is depicted as a dashed line (see text). (c) and (d) $\langle\cos^2\theta\rangle(t)$ (O_2) and $\langle\cos^2\theta\rangle(t)$($N_2$) for calculation shown in (b).

has been determined by analyzing the signal amplitude versus z.[17] The probe beam profile has been measured experimentally by detuning the analyzer with the pump beam off. The measurement, shown as a dashed line in Fig. 2(b), has been used in Eq. 6. The adjustment of the peak intensity $I_{0\mathrm{p}}$ modifies the degree of alignment induced by the pump pulse and therefore the quantities $\langle\cos^2\theta\rangle_i$ in Eq. 6. We emphasize that a modification of the intensity leads to a modification of the alignment transient shape. As already mentioned, the beam waist w_{0x} reflects the spatial averaging due to the propagation of the probe beam over the transverse profile of the pump. For the trace displayed in Fig. 2(b), intensity and waist have been adjusted to $I_{0\mathrm{p}}$=72 TW/cm^2 and $w_{0x} \approx 34$ μm consistent with the estimated experimental parameters. The adjustment of the other lines of the image provides similar results. The value 0.7897 of the relative N_2 concentration resulting from the fit of the central

line is close to the expected value of 0.7884. Adjustment of the others lines provides same result as evidenced by Fig. 3. As expected, when the radial z coordinate (i.e. the line number) increases, the pump intensity and thus the signal to noise ratio is smaller. As a result, the accuracy for the peripherical lines is altered. The concentration of a single

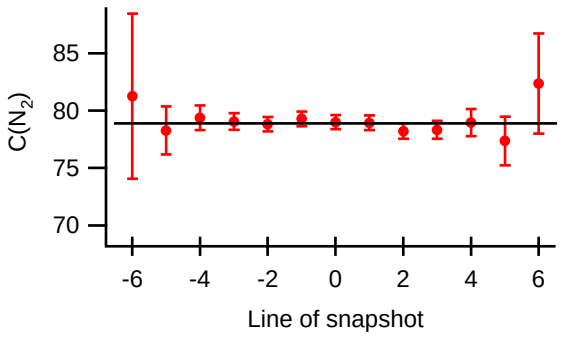

FIG. 3. (Color online) Values of N_2 concentration adjusted from lines -6 to +6 of Fig. 2(a). The errors bars corresponds to three standard deviations and the expected value $C(N_2)$=0.7884 is indicated by the horizontal line.

image is therefore calculated by averaging the concentration of the different lines weighted by the inverse of the standard deviations. In order to validate our method and assess its accuracy, a set of 100 experimental images has been recorded. The averaged value of N_2 and O_2 concentrations are found to be 0.790 $\pm$ 0.004 (one standard deviation) and 0.210 $\pm$ 0.004, respectively. This result is in good agreement with the concentration of atmospheric air, and the uncertainty is only two times the one obtained with a conventional pump-probe method.[15] This finding is particularly interesting in regard of the very short acquisition time (90 ms) of the present investigation and confirms the relevance of the method for fast diagnosis.

V. CONCLUSION

We have determined the concentration of molecular gas mixtures using a spatial imaging technique that measures post-pulse molecular alignment. The method assessed in atmospheric air provides reliable diagnosis on a single-shot basis with a satisfactory accuracy. We emphasize that the present technique can also be extend to other diagnoses like for instance temperature measurement. As the temperature changes, different rotational (or vi-

brational) levels are populated and contribute to the wavepacket whose field-free evolution is thus modified. The temperature can be determined by analysing the transient shape of field-free molecular alignment.[22] We highlight furthermore that the present FTOP technique provides also spatially-resolved diagnoses useful to evaluate inhomogeneous concentration or temperature gradient within the sample. The present technique can be also implemented for investigating collisions in dissipative media. In this case, the major asset of the method is the use of a strong field interaction giving the possibility of measuring the rate characterizing both elastic and inelastic collisions. The collisions manifests themselves as a decay of the birefringence signal with the pump-probe delay. While the transient periodic alignement is sensitive to elastic and inelastic collisions, the permanent alignment (baseline in Fig. 2(b)) is only sensitive to the inelastic one.[14] Finally, in all these issues, the pulse shaping technique could constitute a valuable tool for increasing the degree of molecular alignment[19,23] when required or for improving the diagnosis sensitivity.

ACKNOWLEDGMENTS

This work was supported by the CNRS, the Conseil Régional de Bourgogne, the ANR COMOC, and the FASTQUAST ITN Program of the 7$^{\text{th}}$ FP.

REFERENCES

[1]H. Stapelfeldt and T. Seideman, Rev. Mod. Phys. **75**, 543 (Apr. 2003), http://link.aps.org/abstract/RMP/v75/p543.

[2]F. Rosca-Pruna and M. J. J. Vrakking, Phys. Rev. Lett. **87**, 153902 (Sep. 2001), http://link.aps.org/abstract/PRL/v87/e153902.

[3]V. Renard, M. Renard, S. Guérin, Y. T. Pashayan, B. Lavorel, O. Faucher, and H. R. Jauslin, Phys. Rev. Lett. **90**, 153601 (Apr. 2003), http://link.aps.org/abstract/PRL/v90/e153601.

[4]P. W. Dooley, I. V. Litvinyuk, K. F. Lee, D. M. Rayner, M. Spanner, D. M. Villeneuve, and P. B. Corkum, Phys. Rev. A **68**, 023406 (Aug. 2003), http://link.aps.org/abstract/PRA/v68/e023406.

[5]L. Zhu, K. Suto, J. A. Fiss, R. Wada, T. Seideman, and R. J. Gordon, Phys. Rev. Lett. **79**, 4108 (Nov. 1997), http://link.aps.org/abstract/PRL/v79/p4108.

[6]C. J. Bardeen, V. V. Yakovlev, K. R. Wilson, S. D. Carpenter, P. M. Weber, and W. S. Warren, Chemical Physics Letters **280**, 151 (1997), ISSN 0009-2614, http://www.sciencedirect.com/science/article/B6TFN-3SFVBFC-7J/2/dd54419eaf37367769f00aeacc47d44f.

[7]J. Itatani, J. Levesque, D. Zeidler, H. Niikura, H. Pepin, J. C. Kieffer, P. B. Corkum, and D. M. Villeneuve, Nature **432**, 867 (Dec. 2004), ISSN 0028-0836, http://dx.doi.org/10.1038/nature03183.

[8]N. Wagner, X. Zhou, R. Lock, W. Li, A. West, M. Murnane, and H. Kapteyn, Phys. Rev. A **76**, 061403 (Dec. 2007), http://link.aps.org/abstract/PRA/v76/e061403.

[9]I. V. Litvinyuk, K. F. Lee, P. W. Dooley, D. M. Rayner, D. M. Villeneuve, and P. B. Corkum, Phys. Rev. Lett. **90**, 233003 (Jun. 2003), http://link.aps.org/abstract/PRL/v90/e233003.

[10]D. Pinkham and R. R. Jones, Phys. Rev. A **72**, 023418 (Aug. 2005), http://link.aps.org/abstract/PRA/v72/e023418.

[11]D. Pavicic, K. F. Lee, D. M. Rayner, P. B. Corkum, and D. M. Villeneuve, Phys. Rev. Lett. **98**, 243001 (Jun. 2007), http://link.aps.org/abstract/PRL/v98/e243001.

[12]V. Loriot, E. Hertz, A. Rouzée, B. Sinardet, B. Lavorel, and O. Faucher, Optics Letters **31**, 2897 (Oct. 2006).

[13]V. Loriot, E. Hertz, B. Lavorel, and O. Faucher, Journal of Physics B-atomic Molecular and Optical Physics **41**, 015604 (Jan. 2008).

[14]S. Ramakrishna and T. Seideman, Phys. Rev. Lett. **95**, 113001 (Sep. 2005), http://link.aps.org/abstract/PRL/v95/e113001.

[15]E. Hertz, B. Lavorel, O. Faucher, and R. Chaux, Journal of Chemical Physics **113**, 6629 (Oct. 2000).

[16]E. Hertz, R. Chaux, O. Faucher, and B. Lavorel, Journal of Chemical Physics **115**, 3598 (Aug. 2001).

[17]V. Loriot, R. Tehini, E. Hertz, B. Lavorel, and O. Faucher, Physical Review A **78**, 013412 (Jul. 2008).

[18]M. Fujimoto, S.-i. Aoshima, M. Hosoda, and Y. Tsuchiya, Phys. Rev. A **64**, 033813 (Aug. 2001), http://link.aps.org/abstract/PRA/v64/e033813.

[19]E. Hertz, A. Rouzée, S. Guérin, B. Lavorel, and O. Faucher, Physical Review A **75**, 031403 (Mar. 2007).

[20]E. Hertz, D. Daems, S. Guérin, H. R. Jauslin, B. Lavorel, and O. Faucher, Physical Review A **76**, 043423 (Oct. 2007).

[21]$\Delta\alpha(O_2)$=7.25 u.a, $\Delta\alpha(N_2)$=4.6 u.a.

[22]H. Tran, B. Lavorel, O. Faucher, R. Saint-Loup, and P. Joubert, Journal of Raman Spectroscopy **34**, 994 (2003), http://dx.doi.org/10.1002/jrs.1095.

[23]M. Leibscher, I. S. Averbukh, and H. Rabitz, Phys. Rev. Lett. **90**, 213001 (May 2003), http://link.aps.org/abstract/PRL/v90/e213001.